Attitude dynamics of gyrostat–satellites under control by magnetic actuators at small perturbations

ANTON V. DOROSHIN

Space Engineering Department

Samara National Research University

Moskovskoe shosse 34, Samara, Russian Federation 443086

doran@inbox.ru;   doroshin@ssau.ru

Abstract: - The angular motion of gyrostat-satellites with one axial rotor is considered under control by magnetic actuators and at the action of small polyharmonic perturbations in the own dipole magnetic moment's components which are created proportionally to components of the angular velocity of the satellite. The attitude dynamics is investigated in conditions of the coincidence of the vector of magnetic induction of the external magnetic field and the initial angular momentum vector of the satellite. General and heteroclinic analytical solutions are obtained for dynamical parameters at the relative smallness of the magnetic torques. The chaotic regimes are examined on the base of the Melnikov method and Poincaré sections.

Key-Words: - Satellite; Gyrostat; Dual-Spin Spacecraft; Rigid Body Dynamics; Explicit Exact Solutions; Elliptical Integrals; Jacobi Elliptic Functions; Omega-Maneuver; Heteroclinic chaos; Melnikov function; Poincaré sections

Introduction

The problem of the dynamics analysis of the spacecraft with complex mechanical structure with rotating parts/bodies/equipment (dual-spin spacecraft, multi-spin spacecraft, gyrostat-satellites) and various actuators of control systems always was one of the important part of mechanics and flight dynamics. This problem can be decomposed on many important tasks, starting from the fundamental tasks of classical mechanics of rigid bodies systems [1-5], continuing with new developments in this area [6-8], and focusing on the application of the fundamental results to the analysis of the non-linear regular and chaotic dynamics [9-28] of spacecraft (SC).

The motion of the spacecraft with magnetic control systems was observed and studied in many works in different tasks' formulations [11-28]. In general, the magnetic control technique is based on the interaction of the external magnetic field (the Earth magnetic field, e.g.) and own spacecraft magnetic dipole moment **m**, which is formed by magnetic actuators (magnetic coils and/or rods); and corresponding control lows follow from the controller programs, which generate the concrete time-dependencies of magnetic torque components relatively the connected SC's coordinates frame. These time-dependencies for the components of the SC magnetic dipole moments can have elementary simple or, in contrary, complex shapes. For example, to solve the task of SC attitude stabilization along the local direction of the induction vector of the external magnetic field, we can use the simplest form of the SC own magnetic dipole moment with constant components relatively the connected coordinates frame. Or, in the purposes of decreasing the value of the angular momentum of the SC, the well-known "B-dot" maneuver can be fulfilled [27, 28], when the components of the own SC magnetic dipole moment are formed by the control system with the help of the SC magnetometers: the magnetometers measure derivatives of values of projections of the induction of the external magnetic filed in the SC connected frame, and the control system form the dipole moment components proportionally (but with the opposite sign) to these measured values. So, many cases of the shape of own SC magnetic dipole moment are applicable in the task of the magnetic attitude control, and, moreover, it is possible to indicate the generically defined control as the following low [16]:

$$\mathbf{m} = \mathbf{m}(\mathbf{q}, \boldsymbol{\omega}) = -\left(\varepsilon^2 k_p \mathbf{q} + \varepsilon k_v \mathbf{I} \boldsymbol{\omega} \right)$$

where k_p, k_v, ε are control constants; $\mathbf{q}$ – is the vector of SC attitude parameters (connected with angles/quaternions); $\mathbf{I}$ – is the SC inertia tensor; $\boldsymbol{\omega}$ – is the angular velocity vector of the SC.

The aim of this research is to obtain analytical solutions for the attitude dynamics of the gyrostat-satellite (GS) with magnetic control, and to investigate chaotic regimes in the dynamics at the presence of small perturbations. In the paper we consider the motion of the three-axial GS with the dynamically symmetrical rotor under control by magnetic actuators that create own GS magnetic dipole moment proportional to the angular velocity of the GS main body

$$\mathbf{m}(\boldsymbol{\omega}) = k\boldsymbol{\omega}$$

and, therefore, this dynamical regime can be defined as "the omega-maneuver".

The main motivation of the indicated above subject matter is to prepare the adequate fundamental basis for further developing control systems based on the magnetic torque. Moreover, as the part of this general problem, it is important to find partial simplified techniques of using this magnetic control in cases of small simple spacecraft/satellites with limited sets of equipment, e.g. in the cases of micro-/nano-satellites [28, 29, 32, 33, 34].

As it is assumed in most important works in this field, the main system model represents the rigid body rotating around the fixed point under the action of the restoring torque, that is quite close to the classical tasks of the heavy top motion (in the Euler case, the Lagrange case, and in the case of Kovalevskaya) and the gyrostat motion. By the same way, in this work is considered the SC, which consists from the main rigid body with the rotator (the second rotor-body), and the "fixed point" is correspond to the SC center of mass (realizing its orbital motion at the independent trajectory motion), but the restoring torque is formed by the interaction between the external geomagnetic field and own internal magnetic induction of the SC (as the well-known compass effect). So, the main state space and the main dynamical parameters include, firstly, dynamical and kinematical parameters containing components of the SC angular velocity and directional cosines of the external magnetic induction vector (these cosines also can be expressed through the Euler angles), and, secondly, the Serret-Andoyer-Deprit canonical coordinates. The first class of the dynamical parameters is appropriate for the angular motion obvious description, and the second class is usually used in the framework of studying the perturbed dynamics of Hamiltonian systems and the chaotic aspects description.

1. Mechanical and mathematical models

Let us consider the GS motion at the fulfilment of two conditions. The first condition defines the smallness of the magnetic moment creation, which does not essentially change the vector of the GS angular momentum. The second condition requires the coincidence of the direction of the GS angular momentum vector with the direction of the induction vector of the external magnetic field. The first condition corresponds to the consideration of the weakly perturbed motion. The second condition can be interpreted as the quite possible circumstance of the GS motion, when its center of mass is located in the appropriate orbital segment with the suitable direction of the magnetic induction vector (fig.1) – as the part of such possible cases, the cylindrical precession regime can be indicated. The cylindrical precession regime is realized when the magnetized GS performs an orbital motion on a circular equatorial orbit of the Earth with the angular momentum of the GS is directed perpendicularly to the orbit's plane [9, 11]. Also such motion is very important for the realization of space missions with the

gyroscopically stabilized stationary attitude motions of the GS with the conservation of the spatial orientation of its longitudinal axes (especially it is important for communication satellites).
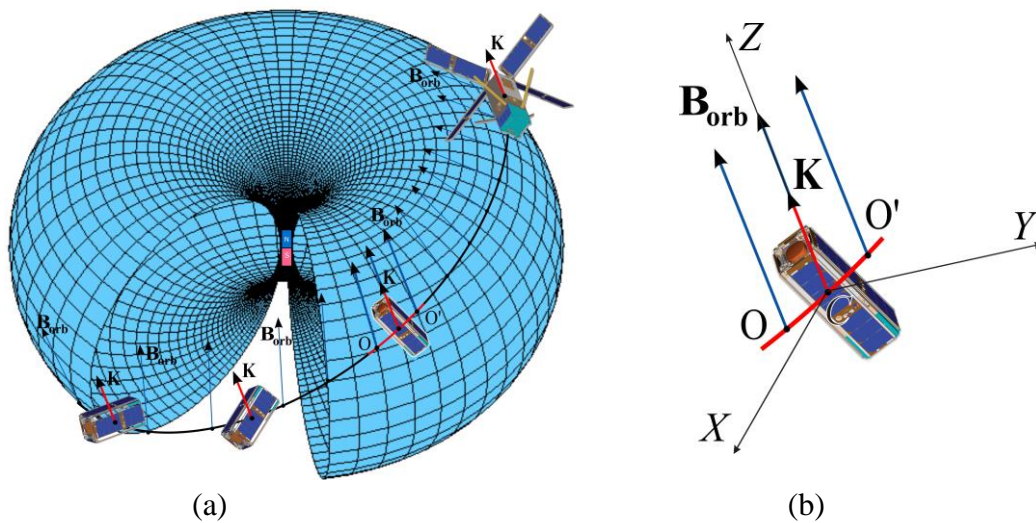

(a)   (b)

Fig.1 – *The model of the Earth's magnetic field and its induction vector* $\mathbf{B}_{orb}$:
(a) – the glide of vectors along the SC[1] orbit; (b) – the main inertial coordinates frame *CXYZ* at the the coincidens of the angular momentum $\mathbf{K}$ with the $\mathbf{B}_{orb}$ direction on the orbit segment OO'

As it is well known, the SC magnetic actuators create the magnetic dipole moment ($\mathbf{m}$), which interacts with the external magnetic field (with the magnetic induction vector $\mathbf{B}_{orb}$) and produce the control torque:

$$\mathbf{M}_{ctrl} = \mathbf{m} \times \mathbf{B}_{orb} \tag{1.1}$$

Let us consider the vector of the external magnetic field induction $\mathbf{B}_{orb}$ as the constant in the inertial space vector. The constancy of the vector $\mathbf{B}_{orb}$ will be quite applicable at the short sector of the orbital SC motion (fig.1).

As it was described above, the own SC magnetic dipole moment can be formed in different complex shapes. In this work we will consider the shape of $\mathbf{m}$ defining the proportionality with the vector $\boldsymbol{\omega}$ of the angular velocity of the main SC body:

$$\mathbf{m} = k\boldsymbol{\omega}, \qquad k = \text{const} \tag{1.2}$$

where in the connected SC coordinates frame *Cxyz* (fig.2) the vector of the angular velocity has the following components: $\boldsymbol{\omega} = [p, q, r]^{\mathrm{T}}$. We can call the motion regime of the SC under control (1.2) when the components of own magnetic dipole moment of the SC are modulated by the control system proportionally to the components of the SC angular velocity vector $\boldsymbol{\omega}$ (1.2) as "the omega-maneuver".

---

[1] The constructional scheme of the SC (GS) depicted at the fig.1 and fig.2 is based on the Multi-Mission Nanosat architecture which was taken from [29].
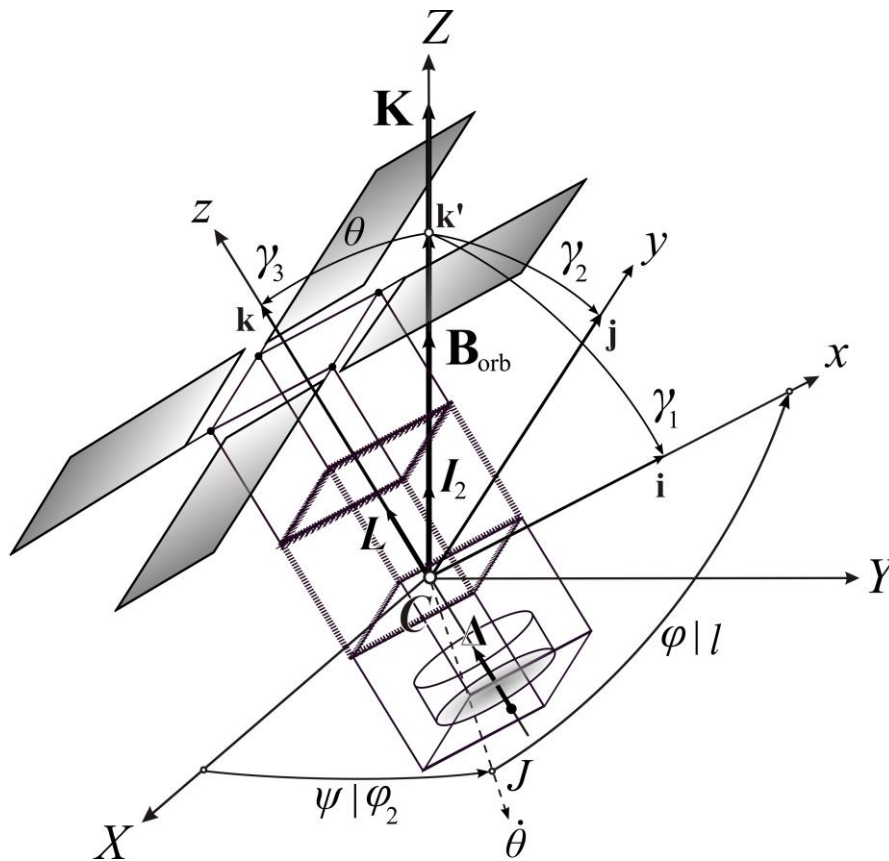
Fig.2 – *The GS schematic construction and coordinates systems*

The main coordinates frames are depicted at the figure (fig.2), including the inertial frame *CXYZ* and the frame *Cxyz* connected with the main body of SC. The inertial axis *CZ* coincides with the constant direction of the vector of the magnetic induction $\mathbf{B}_{orb}$ of the external field – this direction is described by the directional cosines $\gamma_1 = \cos(CZ, Cx)$, $\gamma_2 = \cos(CZ, Cy)$, $\gamma_3 = \cos(CZ, Cz)$, and then we can write the components of the magnetic induction vector $\mathbf{B}_{orb}$ and the magnetic dipole moment $\mathbf{m}$ in the connected coordinates frame *Cxyz*:

$$\mathbf{B}_{orb} = B_{orb}\left[\gamma_1, \gamma_2, \gamma_3\right]^T; \quad \mathbf{m} = k\left[p, q, r\right]^T \qquad (1.3)$$

The motion equations of the SC with one internal rotor-body (that is the GS) with its angular momentum Δ (fig.2) can be written in the vector form of dynamical equations [8-13]:

$$\frac{\tilde{d}}{dt}\mathbf{K} + \boldsymbol{\omega} \times \mathbf{K} = \mathbf{M}_{ctrl} + \mathbf{M}_{add}; \quad \dot{\Delta} = M_{internal} \qquad (1.4)$$

$$\dot{\boldsymbol{\gamma}} = \boldsymbol{\gamma} \times \boldsymbol{\omega} \qquad (1.5)$$

where $\mathbf{M}_{ctrl}$, $\mathbf{M}_{add}$ – are the "controlling" and "additional/disturbing" torques, and $M_{internal}$ – is the value of the internal torque acting on the rotor from the side of the main body, and where the angular momentum of the system $\mathbf{K}$ in projections on axes of the coordinates frame *Cxyz* has the shape:

$$\mathbf{K} = \left[Ap, \ Bq, \ C_b r + \Delta \right]^T \tag{1.6}$$

where $A = A_b + A_r$, $B = B_b + A_r$, $C = C_b + C_r$; A_b, B_b, C_b are the axial inertia moments of the main GS body in the connected frame $Cxyz$; A_r, A_r, C_r are the axial inertia moments of the dynamically symmetrical rotor in its own connected frame. Relatively inertia moments we assume that $A_b > B_b > C_b > A_r > C_r$.

The well-known connections between the Euler angles and the directional cosines (fig.1) have the form:

$$\gamma_1 = \sin\theta \sin\varphi; \quad \gamma_2 = \sin\theta \cos\varphi; \quad \gamma_3 = \cos\theta \tag{1.7}$$

In this research we investigate the GS motion at the absence of the internal interaction between coaxial bodies ($M_{internal}=0$) and, therefore, everywhere below Δ=const. Let us also consider the case of weakly perturbed motion when the value of the magnetic torque is quite small in comparison with angular momentum that is described by the smallness of the dimensionless parameter:

$$\nu = \frac{kB_{orb}}{K} \ll 1 \tag{1.8}$$

and, therefore, it is possible to consider the vector of the angular momentum as practically constant vector $\left(\mathbf{K} \cong \overrightarrow{\text{const}} \right)$. Moreover, let us study the case when the coincidence of the vector $\mathbf{B}_{orb}$ and the angular momentum $\mathbf{K}$ is present (fig.1, fig.2), at least on the initial time-moment of the motion investigation, when the GS is placed into the appropriate segment OO' of the orbit (or the cylindrical precession regime is realized):

$$\mathbf{B}_{orb} = \frac{B_{orb}}{K} \mathbf{K} \tag{1.9}$$

Then considering (1.3), (1.8) and (1.9), the magnetic torque and directional cosines will have the form:

$$\mathbf{M}_{ctrl} = \nu \boldsymbol{\omega} \times \mathbf{K} \tag{1.10}$$

$$\gamma_1 = Ap/K; \quad \gamma_2 = Bq/K; \quad \gamma_3 = (C_b r + \Delta)/K \tag{1.11}$$

Assume that besides the control magnetic torque (1.10), the GS can be at the same time affected by the small additional magnetic torque created by the additional constant magnetic dipole moment $\mathbf{d}$ of the GS, which corresponds, e.g., to the action of the second control contour stabilizing the GS attitude:

$$\mathbf{M}_{add} = \mathbf{d} \times \mathbf{B}_{orb}; \quad \mathbf{d} = \left[0, 0, \tilde{m}_z \right]^T; \tag{1.12}$$

Considering the condition (1.9), the torque (1.12) takes the form:

$$\mathbf{M}_{add} = \mu \mathbf{e}_z \times \mathbf{K} \tag{1.13}$$

with the small parameter

$$\mu = \frac{\tilde{m}_z B_{orb}}{K} << 1 \tag{1.14}$$

As it was assumed above, we suppose that the external torque are small and do not practically change the vector of the angular momentum $\mathbf{K}$. In this case, the motion equations (1.4) can be written in vector and scalar forms:

$$\frac{\tilde{d}}{dt}\mathbf{K} + \boldsymbol{\omega} \times \mathbf{K} = \left[\nu \boldsymbol{\omega} + \mu \mathbf{e}_z \right] \times \mathbf{K} \tag{1.15}$$

$$\begin{cases} A\dot{p} + \left[\left(C_b - B \right) qr + q\Delta \right] \left(1 - \nu \right) = -B\mu q \\ B\dot{q} + \left[\left(A - C_b \right) pr - p\Delta \right] \left(1 - \nu \right) = A\mu p \\ C_b\dot{r} + \dot{\Delta} + pq \left(B - A \right) \left(1 - \nu \right) = 0 \\ \dot{\Delta} = 0 \end{cases} \tag{1.16}$$

The derived equations (1.16) represent the important special case of dynamical equations describing the SC attitude dynamics in the geomagnetic field at the implementation of the cylindrical precession regime. Moreover, these equations correspond to the closed form of differential equations and, therefore, the explicit exact solution can be found, that in its turn is the main aim of this work. So, in the next section, the indicated exact solution is obtaining, and as it will shown at the end of the next section, this solution differs from the previous results for the free gyrostat motion and some perturbed cases [9].

2. The analytical solutions of the motion dynamical equations

2.1. *The general solutions*

Basing on the differential equations (1.16), which we consider as "exact" equations, it is possible to obtain the exact analytical solutions, following to the solution way [9]. From the combination of the dynamical equations (1.16) (the first equation (1.16) is multiplied by p, the second – by q, the third – by r, and the corresponding results are summarized) expression of the kinetic energy conservation follows:

$$A\dot{p}p + B\dot{q}q + C_b\dot{r}r = -\left(B - A \right) \mu pq \tag{1.17}$$

Considering the third equation (1.16) we can express the block from the right part of (1.17)

$$pq(A-B) = \frac{1}{(1-\nu)}\frac{d}{dt}[C_b r + \Delta] \tag{1.18}$$

and the formula (1.17) takes the form in complete differentials

$$\frac{1}{2}\frac{d}{dt}(Ap^2 + Bq^2 + C_b r^2) = \frac{\mu}{(1-\nu)}\frac{d}{dt}[C_b r + \Delta] \tag{1.19}$$

The integration of last expression (1.19) gives the so-called first integral of the energy:

$$Ap^2 + Bq^2 + C_b r^2 + \frac{\Delta^2}{C_r} - \frac{2\mu}{(1-\nu)}[C_b r + \Delta] = 2\tilde{T} \tag{1.20}$$

where

$$\tilde{T} = T_0 - Q\frac{C_2 r_0 + \Delta}{K(1-\nu)} = \text{const}; \quad Q = -EK; \quad E = -\mu;$$

$$2T_0 = Ap_0^2 + Bq_0^2 + C_2 r_0^2 + \frac{\Delta^2}{C_1} = \text{const}; \quad D = \frac{K^2}{2\tilde{T}} = \text{const}$$

The expression for the angular momentum conservation can be written with the help of equations combination (the first equation (1.16) is multiplied by Ap, the second – by Bq, the third – by $(C_b r + \Delta)$, and the corresponding results are summarized and integrated):

$$A^2 p^2 + B^2 q^2 + [C_b r + \Delta]^2 = \text{const} = K^2 = 2D\tilde{T} \tag{1.21}$$

where constant D links the values of the kinetic energy and the angular momentum.

After multiplying (1.20) by A and deducting (1.21) we obtain:

$$B(A-B)q^2 + A\left(C_b r^2 + \frac{\Delta^2}{C_r} + \frac{2E}{(1-\nu)}[C_b r + \Delta]\right) - [C_b r + \Delta]^2 = 2\tilde{T}(A-D) \tag{1.22}$$

After multiplying (1.20) by B and deducting (1.21) we find:

$$A(B-A)p^2 + B\left(C_b r^2 + \frac{\Delta^2}{C_r} + \frac{2E}{(1-\nu)}[C_b r + \Delta]\right) - [C_b r + \Delta]^2 = 2\tilde{T}(B-D) \tag{1.23}$$

It is possible to extract the complete squares in the expressions (1.23), (1.22) and to write them in the form:

$$-A(A-B)p^2 + C_b(B-C_b)\left[r - \frac{\Delta - E(1-v)^{-1}B}{B-C_b}\right]^2 = F \tag{1.24}$$

$$B(A-B)q^2 + C_b(A-C_b)\left[r - \frac{\Delta - E(1-v)^{-1}A}{A-C_b}\right]^2 = H \tag{1.25}$$

where

$$F = 2\tilde{T}(B-D) + \frac{C_b}{B-C_b}\left(\Delta - \frac{E}{(1-v)}B\right)^2 - \left[\left(\frac{B}{C_r}-1\right)\Delta^2 + 2\frac{E}{(1-v)}B\Delta\right];$$

$$H = 2\tilde{T}(A-D) + \frac{C_b}{A-C_b}\left(\Delta - \frac{E}{(1-v)}A\right)^2 - \left[\left(\frac{A}{C_r}-1\right)\Delta^2 + 2\frac{E}{(1-v)}A\Delta\right] \tag{1.26}$$

Then from (1.24) and (1.25) the expressions follow

$$p = \pm\sqrt{\frac{C_b(B-C_b)\left[r - \frac{\Delta - E(1-v)^{-1}B}{B-C_b}\right]^2 - F}{A(A-B)}};$$

$$r - \frac{\Delta - E(1-v)^{-1}A}{A-C_b} = \pm V(q); \quad r - \frac{\Delta - E(1-v)^{-1}B}{B-C_b} = \pm V(q) - \Delta\beta - \frac{E\alpha}{(1-v)}; \tag{1.27}$$

where

$$V(q) = \sqrt{\frac{H - B(A-B)q^2}{C_b(A-C_b)}}; \quad \beta = \frac{A-B}{(B-C_b)(A-C_b)}; \quad \alpha = \frac{(B-A)C_b}{(B-C_b)(A-C_b)}$$

The third equation can be rewritten in the explicit factorized shape

$$B\dot{q} = \mp(1-v)(A-C_b)W(q)V(q) \tag{1.28}$$

where

$$W(q) = \sqrt{\frac{C_b(B-C_b)}{A(A-B)}\left[\pm V(q) - \Delta\beta - \frac{E}{(1-v)}\alpha\right]^2 - \frac{F}{A(A-B)}};$$

With the help of the change of variables [9]

$$x = \pm V(q) - \Delta\beta - \frac{E}{(1-v)}\alpha \tag{1.29}$$

the equation (1.28) takes the form with separated differentials

$$dt = \pm \frac{M}{(1-v)\sqrt{ac}} \frac{dx}{\sqrt{\left(\sqrt{\frac{H}{a}}\right)^2 - (x+b)^2}\sqrt{x^2 - \left(\sqrt{\frac{G}{c}}\right)^2}} \tag{1.30}$$

where constants and initial values have the following values

$$M = C_2 \sqrt{\frac{B}{A-B}}; \quad G = \frac{F}{A(A-B)}; \quad a = C_b(A-C_b); \quad b = \Delta\beta + \frac{E}{(1-v)}\alpha; \quad c = \frac{C_b(B-C_b)}{A(A-B)} \tag{1.31}$$

$$x(t_0) = x_{ini} = \pm\sqrt{\frac{H - B(A-B)q_0^2}{C_b(A-C_b)} - \Delta\beta - \frac{E}{(1-v)}\alpha} \tag{1.32}$$

After the second change of the variables the equation (1.30) takes the form

$$dt = \pm 2eM \frac{\sqrt{R/P}}{(1-v)\sqrt{aG}}\left[\sqrt{s_2 s_4}\sqrt{\left(1-\frac{z^2}{c_1^2}\right)\left(1-\frac{z^2}{c_2^2}\right)}\right]^{-1} dz; \qquad z = \sqrt{\frac{R(x-e)}{P(x+e)}}; \tag{1.33}$$

where

$$R = -b-d+e; \quad P = -b-d-e; \quad d = \sqrt{H/a}; \quad e = \sqrt{G/c}; \quad c_1^2 = s_2/s_1; \quad c_2^2 = s_4/s_3;$$

$$s_1 = d+e-b; \quad s_2 = \frac{R}{P}[d-e-b]; \quad s_3 = d-e+b; \quad s_4 = \frac{R}{P}[d+e+b];$$

One more change of variables is needed $(z = \tilde{c}y; \quad \tilde{c} = \min\{c_1, c_2\}; \quad \underset{\sim}{c} = \max\{c_1, c_2\}; \quad k = \tilde{c}/\underset{\sim}{c})$, which allows to integrate the equation (1.33) as the elliptic integral:

$$\pm\left[N(1-v)(t-t_0) + I_0\right] = \int_0^y \frac{dy}{\sqrt{(1-y^2)(1-k^2 y^2)}}; \tag{1.34}$$

where

$$N = \left[2eM \frac{\tilde{c}\sqrt{R/P}}{\sqrt{aG}\sqrt{s_2 s_4}}\right]^{-1}; \quad I_0 = \int_0^{y_0} \frac{dy}{\sqrt{(1-y^2)(1-k^2 y^2)}} = \text{const}$$

After the elliptic integral inversion we obtain the explicit solution [9] as the Jacobi elliptic sine

$$y(t) = \text{sn}\left[\pm\left(N(1-v)(t-t_0) + I_0\right), k\right] \tag{1.35}$$

The back substitutions give the exact explicit expressions for all dynamical parameters

$$\begin{cases} q(t) = \pm\sqrt{\dfrac{1}{B(A-B)}\Big[H - C_b(A-C_b)(x(t)+\Delta\beta)^2\Big]}; \\[2ex] p(t) = \pm\sqrt{\dfrac{1}{A(A-B)}\Big[C_b(B-C_b)x^2(t)-F\Big]}; \\[2ex] r(t) = \dfrac{\Delta}{A-C_b} \pm\left(x(t)+\Delta\beta+\dfrac{E}{(1-v)}\alpha\right); \\[2ex] x(t) = e\dfrac{R/P+\tilde{c}^2\,\mathrm{sn}^2\Big[\pm\big(N(1-v)(t-t_0)+I_0\big),k\Big]}{R/P-\tilde{c}^2\,\mathrm{sn}^2\Big[\pm\big(N(1-v)(t-t_0)+I_0\big),k\Big]}; \end{cases} \qquad (1.36)$$

As can we see, the exact solutions (1.36) of the equations (1.16) differ from the corresponding dependencies for free GS [9] in the part of the frequency of the elliptic function, and if $v=0$ then solutions will be identical relative the previous works [9]. The graphics (Fig. 3) demonstrate the correctness of the analytical solutions (1.36), that corresponds to the coincidence of the analytical calculations (points) and the numerical integration results (lines).
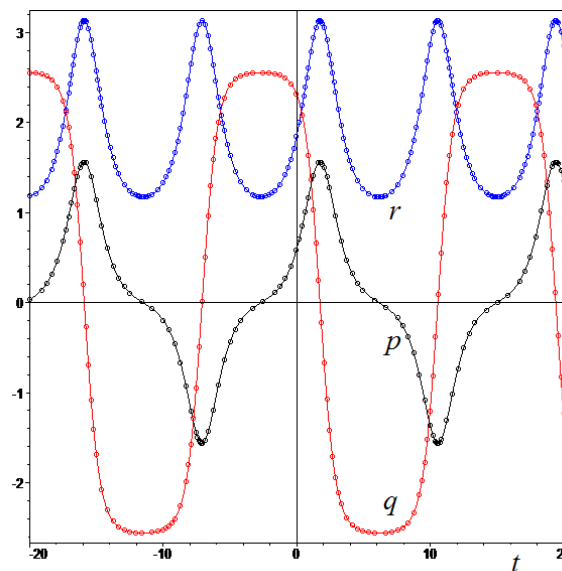
Fig.3 – *The numerical integration (lines) and analytical (points) results (1.36)*
A_b=15, B_b=10, C_b=7, A_r=5, C_r=4 [kg·m²]; p_0=0.60, q_0=2.31, r_0=1.86 [1/s];
Δ=3, K=40 [kg·m²/s]; Q=10 [kg·m²/s²]; μ=-0.25 [1/s]; v=0.30

2.2. *The heteroclinic solutions*

Also it is important to indicate the partial case of the general solution (1.36), which corresponds to the heteroclinic separatrices-polhodes [11] – it realizes at the condition F=0. In this case the elliptic functions reduce to the hyperbolic form (when elliptic module k=1):

$$
\left\{
\begin{aligned}
& \bar{p}(t) = \pm\sqrt{\frac{C_b(B-C_b)}{A(A-B)}}\,\bar{x}(t); \quad \bar{q}(t) = \pm\sqrt{\varsigma^2 - \chi^2\left(\bar{x}(t)+\Delta\beta+\frac{E}{(1-v)}\alpha\right)^2}; \\[2mm]
& \bar{r}(t) = \bar{x}(t) + \frac{\Delta - \dfrac{E}{(1-v)}B}{B-C_b}; \quad \bar{x}(t) = \frac{4a_0\Phi_0\exp\left(\mp\dfrac{\tilde{M}\sqrt{a_0}}{\chi^2}(1-v)t\right)}{\left[\Phi_0\exp\left(\mp\dfrac{\tilde{M}\sqrt{a_0}}{\chi^2}(1-v)t\right)-a_1\right]^2 - 4a_2a_0}
\end{aligned}
\right.
\tag{1.37}
$$

where

$$
\Delta = \text{const} > 0; \quad a_2 = -\chi^2; \quad a_1 = -2\left(\Delta\beta+\frac{E}{(1-v)}\alpha\right)\chi^2; \quad a_0 = \varsigma^2 - \chi^2\left(\Delta\beta+\frac{E}{(1-v)}\alpha\right)^2;
$$

$$
\varsigma^2 = \frac{\tilde{H}}{B(A-B)}; \quad \chi^2 = \frac{C_b(A-C_b)}{B(A-B)}; \quad \tilde{M} = \frac{(A-C_b)}{B}\sqrt{\frac{C_b(B-C_b)}{A(A-B)}};
$$

$$
\tilde{H} = 2\tilde{T}(A-\tilde{D}) + \frac{C_b}{A-C_b}\left(\Delta-\frac{E}{(1-v)}A\right)^2 - \left[\left(\frac{A}{C_r}-1\right)\Delta^2 + 2\frac{E}{(1-v)}A\Delta\right];
$$

$$
\tilde{D} = B + \frac{1}{2\tilde{T}}\left(\frac{C_b}{B-C_b}\left(\Delta-\frac{E}{(1-v)}B\right)^2 - \left[\left(\frac{B}{C_r}-1\right)\Delta^2 + 2\frac{E}{(1-v)}B\Delta\right]\right);
$$

$$
E = -\mu; \quad Q = \mu K; \quad \tilde{T} = T_0 - Q\frac{C_2r_0+\Delta}{K(1-v)} = \text{const}; \quad 2T_0 = Ap_0^2 + Bq_0^2 + C_br_0^2 + \frac{\Delta^2}{C_r};
$$

$$
\Phi_0 = \Phi(y_0^\pm); \quad \Phi(z) = \frac{1}{z}\left(2a_0 + a_1z + 2\sqrt{a_0}\sqrt{a_2z^2+a_1z+a_0}\right); \quad y_0^\pm = \pm\frac{\varsigma}{\chi} - \left(\Delta\beta+\frac{E}{(1-v)}\alpha\right)
$$

The correctness of the solutions (1.37) is checked by the coincidence with the corresponding numerical integration results (fig.4). These solutions can be very important at the research of the chaotic dynamics [e.g., 10-13, 17, 31].
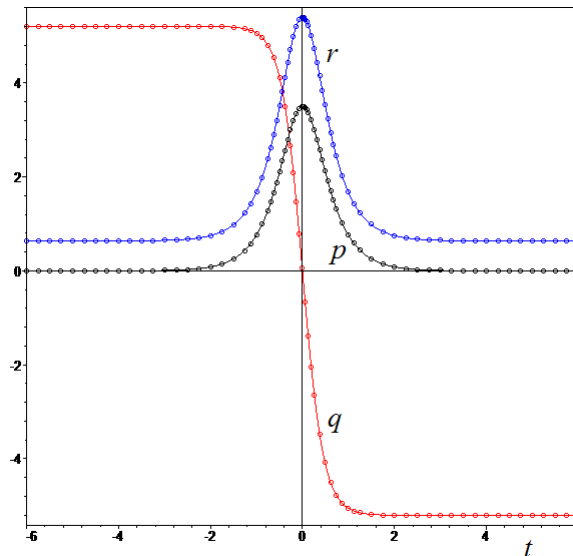
Fig.4 – *The numerical integration (lines) and analytical (points) results (1.37)*
A_b=15, B_b=10, C_b=6, A_r=5, C_r=4 [kg·m²]; p_0=3.5, q_0=0, r_0=5.4 [1/s];
Δ=3, K=78.44 [kg·m2/s]; Q=10 [kg·m²/s²]; μ=-0.13 [1/s]; ν=0.30

2.3. *The additional partial case of the heteroclinic solutions*

In purposes of the simplest form of heteroclinic solution obtaining, let us consider the GS motion at the same main conditions that were described above in the subsection 2.2, but also at the fulfillment of some additional requirements. Assume that besides the action of small torques (1.10) and (1.13), the GS motion fulfills at the following combination of parameters:

$$\Delta(1-\nu)+C_b\mu = 0 \tag{1.38}$$

This additional condition can be implemented with the help of the control system of magnetic actuators, and/or by the change of the value of the rotor internal angular momentum Δ. At the fulfillment of the requirement (1.38) the equations (1.16) take the shape:

$$\begin{cases} A\dot{p}+(C_b-B)q[r+\tilde{\mu}](1-\nu)=0 \\ B\dot{q}+(A-C_b)p[r+\tilde{\mu}](1-\nu)=0 \\ C_b\dot{r}+pq(B-A)(1-\nu)=0 \end{cases} \tag{1.39}$$

where $\tilde{\mu}=\mu/(1-\nu)$.

The equations (1.39) will have the partial solution in the following qualitative form:

$$\overline{p}(t)=p_0/\mathrm{ch}\,\lambda t; \quad \overline{q}(t)=\rho\,\mathrm{th}\,\lambda t; \quad \overline{r}(t)=\frac{r_0+\tilde{\mu}}{\mathrm{ch}\,\lambda t}-\tilde{\mu}; \tag{1.40}$$

where initial values p_0 and r_0 satisfy the condition (1.24) of the heteroclinic separatrices-polhodes realization (at F=0) and $\{\rho, \lambda\}$ are unknown constant parameters. The solution (1.40) represents the partial case of the heteroclinic solution (1.37), and it has the simplest shape described by the simplest

hyperbolic functions. To obtain the correct final form of this solutions we need to substitute formulas (1.40) directly into the equations (1.39). Using properties of the symmetry of the derivations of hyperbolic functions:

$$\dot{p} = -p_0 \lambda \frac{\operatorname{sh} \lambda t}{\operatorname{ch}^2 \lambda t}; \quad \dot{q} = \lambda \rho \frac{1}{\operatorname{ch}^2 \lambda t}; \quad \dot{r} = -(r_0 + \tilde{\mu}) \lambda \frac{\operatorname{sh} \lambda t}{\operatorname{ch}^2 \lambda t}$$

the substitution gives the following algebraic nonlinear equations:

$$\begin{cases} -A\lambda p_0 + (C_b - B)\rho[r_0 + \tilde{\mu}](1-\nu) = 0 \\ B\lambda\rho + (A - C_b)p_0[r_0 + \tilde{\mu}](1-\nu) = 0 \\ -C_b\lambda[r_0 + \tilde{\mu}] + (B - A)\rho p_0(1-\nu) = 0 \end{cases} \tag{1.41}$$

From the system (1.41) it is possible to find the expressions:

$$\rho^2 = \frac{(C_b - A)A}{(C_b - B)B} p_0^2; \quad \lambda^2 = \frac{(C_b - A)(B - A)}{BC_b} p_0^2 \tag{1.42}$$

Taking into account (1.38), the condition (1.24) of the heteroclinic separatrices-polhodes realization takes the form (that corresponds to *F=0*):

$$A(A - B) p_0^2 = C_b(B - C_b)\left[r_0 + \frac{\Delta}{C_b}\right]^2 \tag{1.43}$$

The last condition (1.43) allows to write four cases (*i·j*, *i=1..2*, *j=1..2*) of the initial conditions combination:

$$r_0 = f(p_0) = \frac{(-1)^i \sqrt{A(A-B)} p_0}{(-1)^j \sqrt{C_b(B-C_b)}} - \frac{\Delta}{C_b} \tag{1.44}$$

So, basing on the initial values (1.44) and parameters (1.42), we have the fully defined simplest heteroclinic solution (1.40) at the predefined (arbitrary) value p_0.

3. The canonical form of the dynamical model in the Serret-Andoyer-Deprit variables

Let us involve the very important and useful form of the dynamical model, which is based on the Hamiltonian mechanics, and can be applied to the investigation of the nonlinear phenomena of the dynamics, including homo/heteroclinic chaos initializing. As the canonical variables in this work the well-known [3-6] canonical pares of the Serret-Andoyer-Deprit variables ($\{\varphi_3, I_3\}, \{\varphi_2, I_2\}, \{l, L\}$) are used:

$$L = \frac{\partial T}{\partial \dot{l}} = \mathbf{K} \cdot \mathbf{k}; \quad I_2 = \frac{\partial T}{\partial \dot{\varphi}_2} = \mathbf{K} \cdot \frac{\mathbf{K}}{K} = |\mathbf{K}| = K; \quad I_3 = \frac{\partial T}{\partial \dot{\varphi}_3} = \mathbf{K} \cdot \mathbf{k}' \tag{2.1}$$

In the considering case (when $\mathbf{K}\uparrow\uparrow CZ$) the canonical variables reduce to two pares ($\{\varphi_2, I_2\},\{l, L\}$) that depicted at the fig.2, and the correspondences with the Euler angles are actual:

$$\left\{ \begin{array}{l} l = \varphi; \quad \varphi_2 = \psi; \quad \varphi_3 = 0; \\[2mm] I_2 = K; \quad \cos\theta = \dfrac{L}{I_2} = \dfrac{L}{K}; \\[2mm] \sin\theta = \dfrac{\sqrt{I_2^2 - L^2}}{I_2} = \dfrac{\sqrt{K^2 - L^2}}{K} \end{array} \right. \tag{2.2}$$

The angular momentum components are linked with the canonical momentums as follows:

$$K_x = Ap = \sqrt{I_2^2 - L^2}\,\sin l; \quad K_y = Bq = \sqrt{I_2^2 - L^2}\,\cos l; \quad K_z = C_b r + \Delta = L \tag{2.3}$$

As it is considered in previous works [e.g., 11-13], the Hamiltonian of the GS system in the Serret-Andoyer–Deprit variables has the form:

$$\mathcal{H} = \mathcal{H}_0 + \varepsilon\mathcal{H}_1; \quad \mathcal{H}_0 = T + P;$$
$$T = \frac{I_2^2 - L^2}{2}\left[\frac{\sin^2 l}{A} + \frac{\cos^2 l}{B}\right] + \frac{1}{2}\left[\frac{\Delta^2}{C_r} + \frac{(L-\Delta)^2}{C_b}\right] \tag{2.4}$$

where T is the kinetic energy, P is the potential energy, and $\varepsilon\mathcal{H}_1$ − is the part of the Hamiltonian which describes possible small (proportional to the small parameter ε) perturbations acting on the system. To write the expressions for the potential energy it is needed to consider the magnitude of the magnetic torque (1.1) with integrating it by the corresponding positional angle $\vartheta = \angle(\mathbf{m}, \mathbf{B}_{orb})$:

$$\left|\mathbf{M}_{ctrl}\right| = \left|\mathbf{m} \times \mathbf{B}_{orb}\right| = \left|\mathbf{m}\right|\left|\mathbf{B}_{orb}\right|\sin\vartheta;$$
$$P = -\int\left|\mathbf{M}_{ctrl}\right|d\vartheta = -\left|\mathbf{m}\right|\left|\mathbf{B}_{orb}\right|\cos\vartheta = -\mathbf{m}\cdot\mathbf{B}_{orb} = -B_{orb}\mathbf{m}\cdot\boldsymbol{\gamma} = \tag{2.5}$$
$$= -B_{orb}\left[\sin\theta\left(m_x\sin\varphi + m_y\cos\varphi\right) + m_z\cos\theta\right]$$

Then the potential energy (2.5) in the Serret-Andoyer-Deprit variables can be obtained with the help of connections (2.2)

$$P = -B_{orb}\left[\frac{\sqrt{I_2^2 - L^2}}{I_2}\left(m_x\sin l + m_y\cos l\right) + m_z\frac{L}{I_2}\right] \tag{2.6}$$

In the considering case, taking in mind shapes of the magnetic dipole components and parameters (1.3) -(1.14), the potential energy can be written in the form:

$$P = -v\left[\left(I_2^2 - L^2\right)\left(\frac{\sin^2 l}{A} + \frac{\cos^2 l}{B}\right) + \frac{(L-\Delta)L}{C_b}\right] - \mu L \qquad (2.7)$$
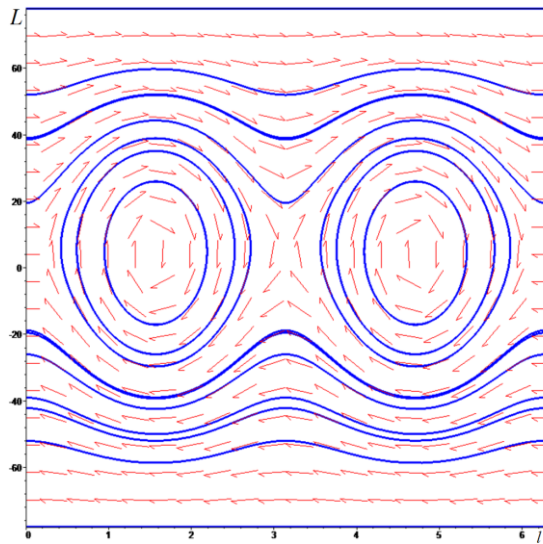
Let us assume the presence of small polyharmonic synchronous oscillations in the both considered dynamical factors (described by the parameters v and μ) of the magnetic dipole value, which expressed in the corresponding parameters change

$$v(t) = v\left(1 + e_v g(t)\right); \quad \mu(t) = \mu\left(1 + e_\mu g(t)\right) \qquad (2.8)$$

where the small multipliers e_v, $e_\mu \ll 1$ and the polyharmonic perturbation with the basic frequency ω_p take place

$$g(t) = \sum_{n=1}^{N}\left[c_n \cos\left(n\omega_p t\right) + s_n \sin\left(n\omega_p t\right)\right] \qquad (2.9)$$

Then the following perturbed part of the Hamiltonian can be written

$$\varepsilon \mathcal{H}_1 = -\varepsilon\left\{\frac{v e_v}{\mu e_\mu}\left[\left(I_2^2 - L^2\right)\left(\frac{\sin^2 l}{A} + \frac{\cos^2 l}{B}\right) + \frac{(L-\Delta)L}{C_b}\right] + L\right\}g(t) \qquad (2.10)$$

where the small parameter is introduced as $\varepsilon = \mu e_\mu$.

As can we see from the Hamiltonian, only the pare $\{l, L\}$ corresponds to the positional coordinates, and others Serret-Andoyer-Deprit variables are cyclic and do not affect the dynamics in the considering case. Then only two canonical equations are important for our consideration:
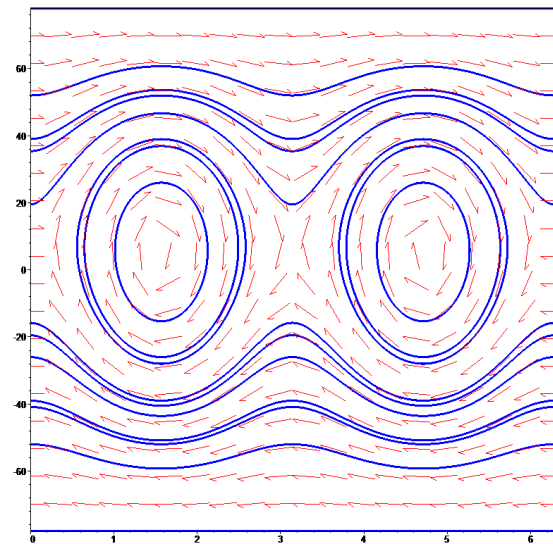
$$\begin{cases} \dot{L} = -(1-2v)\left[I_2^2 - L^2\right]\left(\frac{1}{A} - \frac{1}{B}\right)\frac{\sin(2l)}{2} - \varepsilon\frac{\partial \mathcal{H}_1}{\partial l}; \\ \dot{l} = (1-2v)L\left[\frac{1}{C_b} - \frac{\sin^2 l}{A} - \frac{\cos^2 l}{B}\right] - (1-v)\frac{\Delta}{C_b} - \mu + \varepsilon\frac{\partial \mathcal{H}_1}{\partial L} \end{cases} \qquad (2.11)$$

The equations (2.11) fully describe the system's dynamics; the corresponding phase portraits (PP) of the generating system (without the perturbations, i.e. $\varepsilon=0$) in the space $\{0 \le l \le 2\pi; -K \le L \le K\}$ are presented at the fig.5.
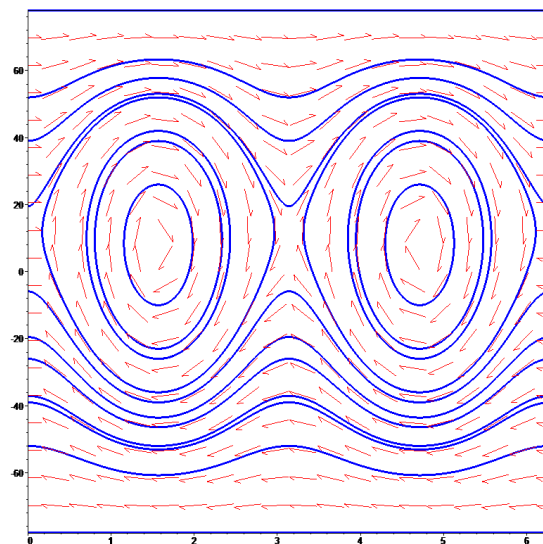
Notwithstanding that the smallness of the parameters v and μ is claimed, it is very important to observe the whole possible bifurcation picture in the system, allowing the broad interval of v and μ values change. Then from the fig.5 the bifurcation scheme follows at rising the value of the v-parameter (on the interval $[-1,1]$): at the frames from (a): $v=-1$ to (e): $v=0.4$ the first PP-type and its serial deformation are depicted; beginning from the frame (j): $v=0.54$ and up to the frame (o): $v=0.9$ the second PP-type is shown with its sequential change; at the frame (f): $v=0.45$ and up to (i): $v=0.535$ we see the transitional PP-type takes place; the frame (p): $v=1.0$ corresponds to the degeneration of the phase portrait. So, the demonstrated bifurcation serial reconstruction at the variation of the v-parameter can be quite useful in the framework of the GS attitude control and/or dynamical regimes switching.
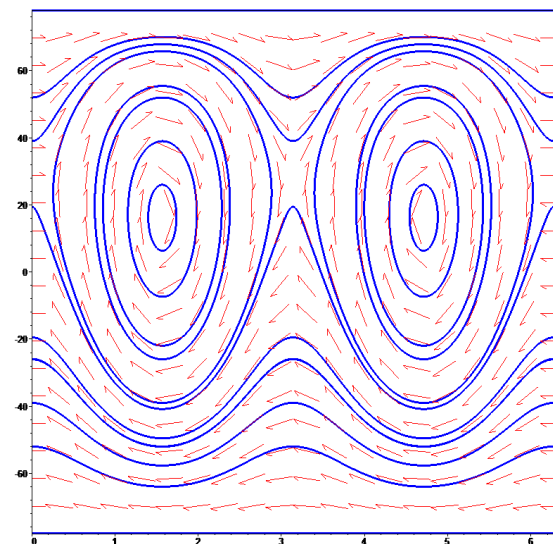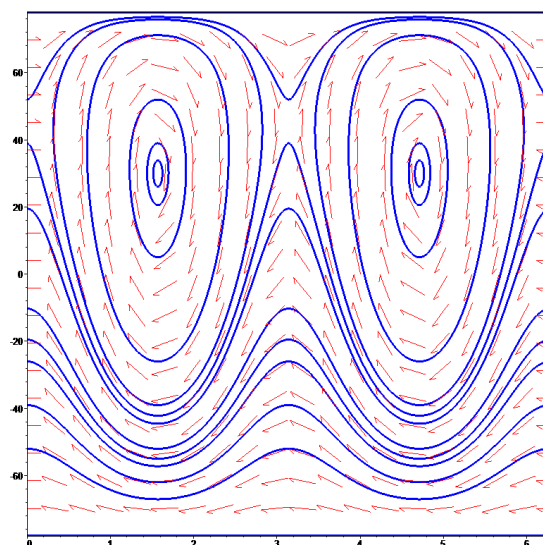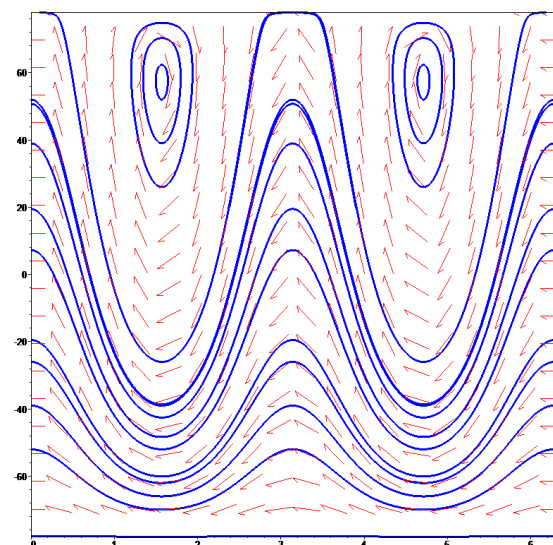
(a) *v*=-1

(b) *v*=-0.5

(c) *v*=0

(d) *v*=0.3

(e) *v*=0.4

(f) *v*=0.45

(g) *v*=0.5

(h) *v*=0.53

(i) *v*=0.535

(j) *v*=0.54

(k) *v*=0.55

(l) *v*=0.57

(m) v=0.6 (n) v=0.8

(o) v=0.9 (p) v=1.0
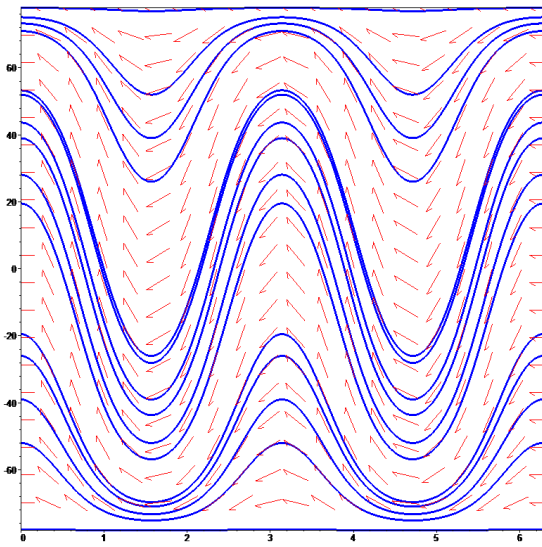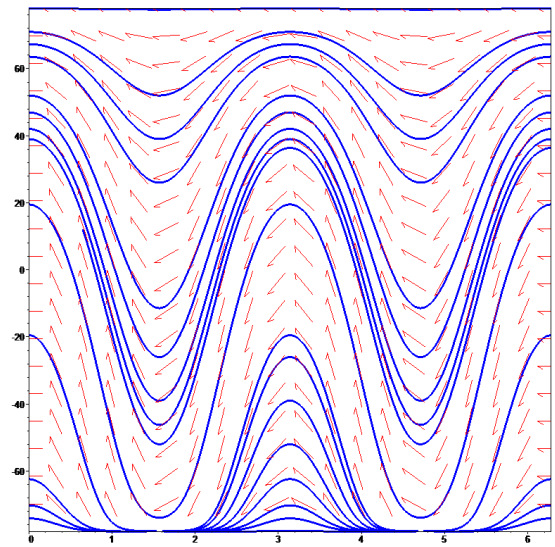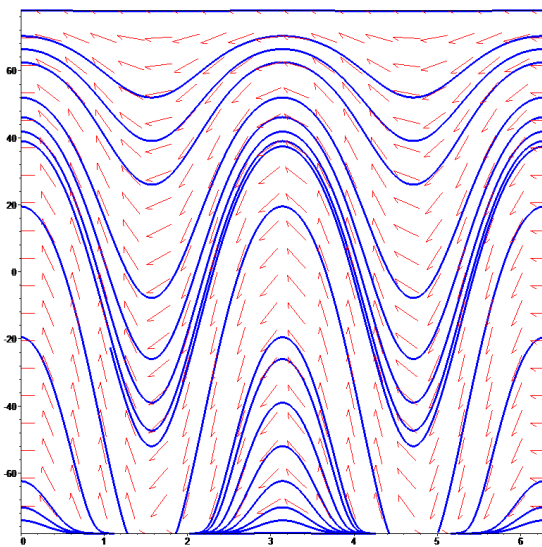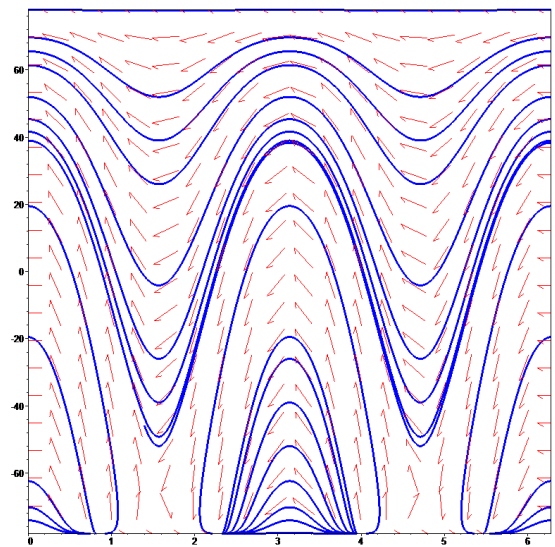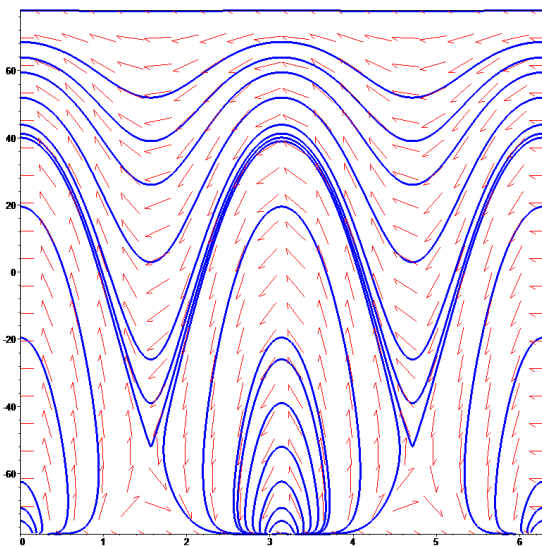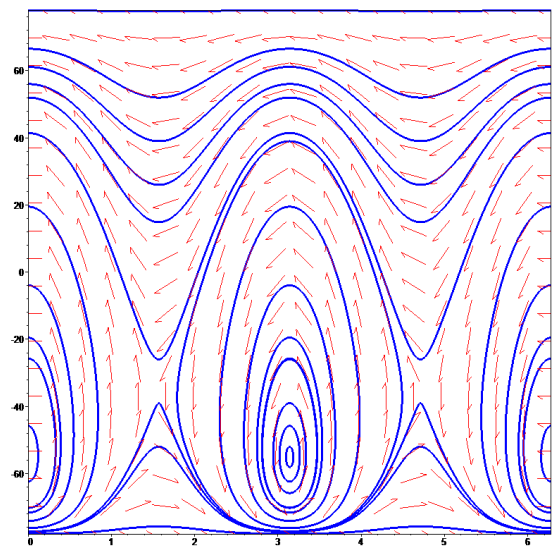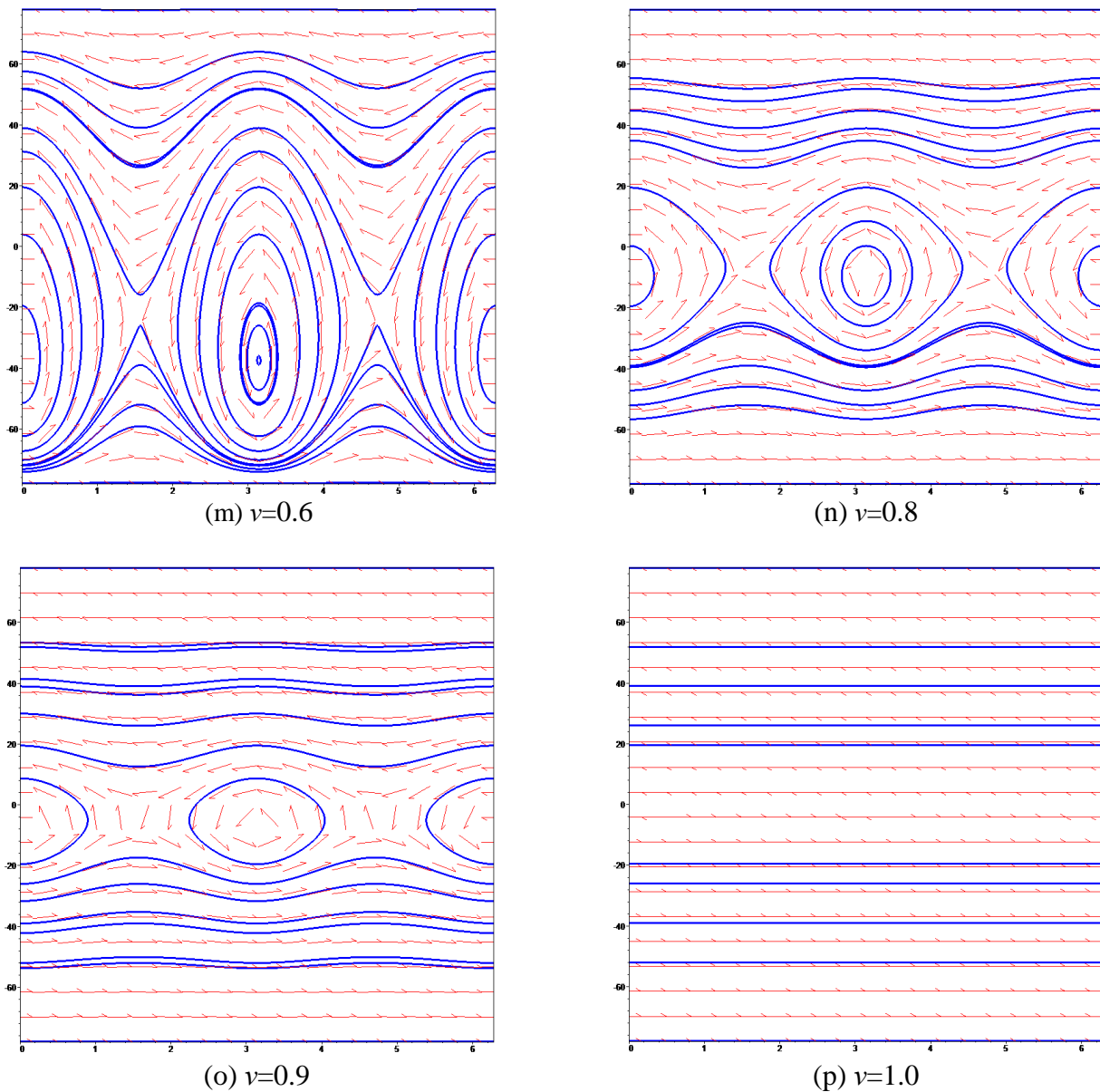
Fig.5 – *The phase portraits {l, L} of the GS system at the change of the v-parameter*
A=15, B=10, C_b=6 [kg·m^2]; Δ=3, K=78 [kg·m2/s]; μ=0.3 [1/s]; ε=0

In the continuation of the bifurcation scheme investigating it is needed to present the PP deformations at rising the value of the μ-parameter (fig.6). As can we see (fig.6), the PP is gradually moving up (frame b), changes the type (frame c), and degrades at following μ-parameter rising (frame d). Also it is important to note that at decreasing the μ-parameter (to negative values) the similar PP-deformation takes place, but the picture is moving down. Such scheme of the PP bifurcation is also typical for the case of the gyrostatic angular momentum Δ variation [e.g. 8, 10].

So, the fundamental bifurcation picture basing on the considered schemes (fig.5, fig.6) can be applied to the GS attitude control and dynamical regimes changing. Here, however, we have to note that variation intervals for the "magnetic" parameters (v and μ) should be selected in view of requirements of the smallness of magnetic perturbations, which defines the applicability of the main equations (2.11) and (1.16) itself.
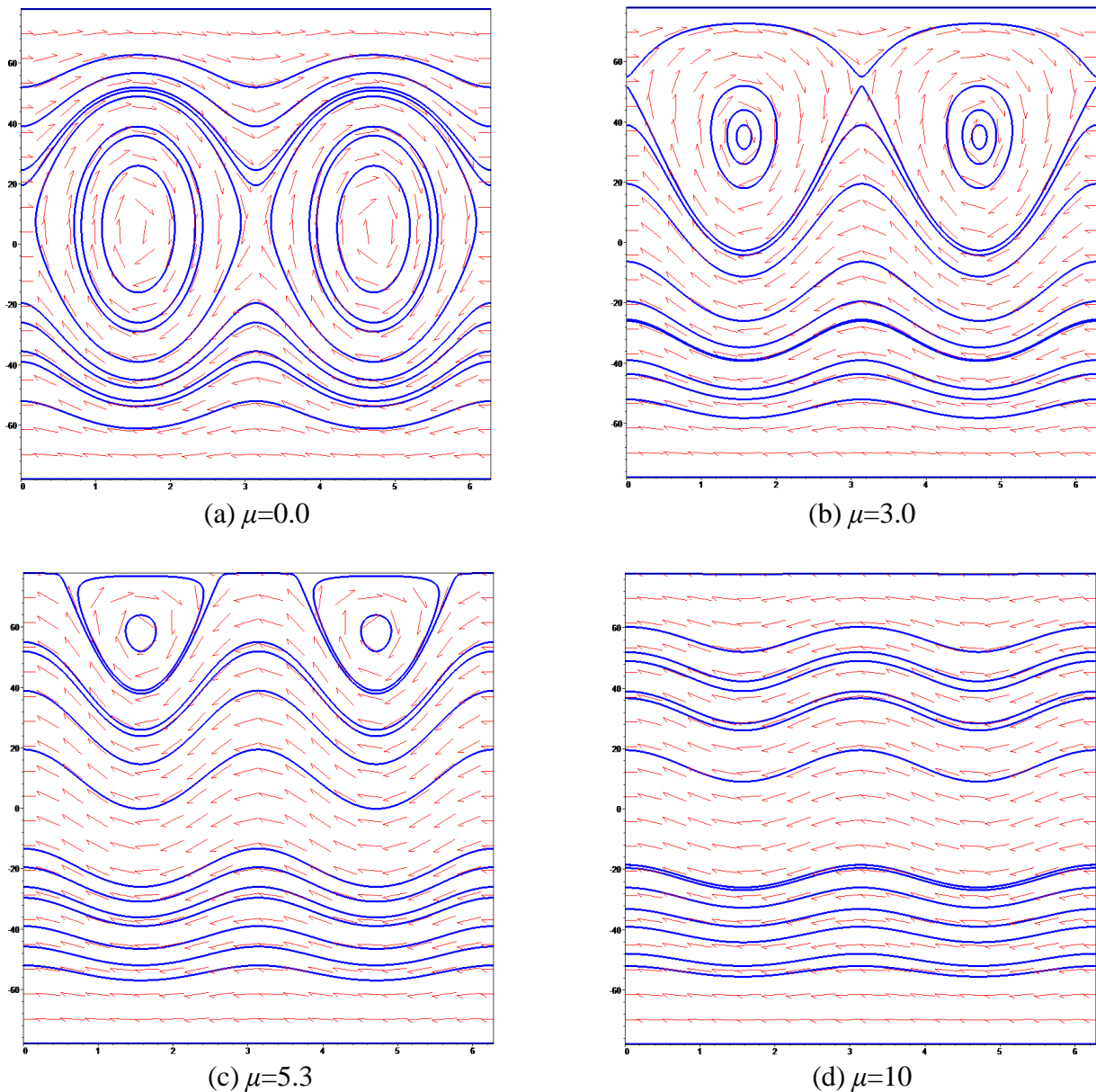
(a) μ=0.0

(b) μ=3.0

(c) μ=5.3

(d) μ=10

Fig.6 – *The phase portraits {l, L} of the GS systems at the change of the μ-parameter*
A=15, B=10, C_b=6 [kg·m²]; Δ=3, K=78 [kg·m2/s]; v=0; ε=0

4. The perturbed dynamics and the heteroclinic chaos initiation

Let us fulfill the short modelling of the GS dynamics at the presence of the perturbations defined by the Hamiltonian (2.4) (with the potential energy (2.7)) and its perturbed part (2.10). Firstly, it is easy to evaluate the well-known Melnikov function, which can analytically show the possibility of the chaotic dynamics initiation near homo/heteroclinic regions. In the considering case the perturbed part of the Hamiltonian depends only on the pare of {l, L} variables and t, and, therefore the classical Melnikov function can be applied [30]:

$$M\left(t_0\right) = \varepsilon \int_{-\infty}^{+\infty} \left[\frac{\partial \mathcal{H}_0}{\partial l} \frac{\partial \mathcal{H}_1}{\partial L} - \frac{\partial \mathcal{H}_0}{\partial L} \frac{\partial \mathcal{H}_1}{\partial l} \right]_{(\bar{l}(t), \bar{L}(t), t+t_0)} dt \qquad (2.12)$$

where the subscription $\left(\bar{l}\left(t\right), \bar{L}\left(t\right), t+t_0 \right)$ indicates that the generating heteroclinic solutions must be substituted into the integral structure. Taking into account the correspondences (2.3) and heteroclinic solutions (1.37) (or (1.40)), the Melnikov function is written in the shape:

$$M\left(t_0\right) = 2\varepsilon AB \left(\frac{1}{A} - \frac{1}{B} \right) \int_{-\infty}^{+\infty} \bar{p}(t)\bar{q}(t)\Omega(t) g\left(t+t_0\right) dt; \tag{2.13}$$

where

$$\left\{ \begin{aligned} &\Omega(t) = \Phi + \Lambda(t); \\ &\Phi = \left\{ \mu\left[(1-\nu)e_\mu - 2\nu e_\nu\right] + \frac{\Delta}{C_b}\left[\nu e_\nu(1-\nu)\right] \right\} = \text{const}; \\ &\Lambda(t) = \left(C_b\bar{r}(t) + \Delta\right)\left(\frac{1}{C_b} - \frac{A\bar{p}^2(t) + B\bar{q}^2(t)}{I_2^2 - \left(C_b\bar{r}(t) + \Delta\right)^2} \right)\left\{ 2\nu e_\nu(2-3\nu) \right\} \end{aligned} \right. \tag{2.14}$$

Now it is important to analyze the internal structure of the integral (2.13). Having regard to the solutions (1.37) (or (1.40)), we can conclude that functions $\Lambda(t)$ and $\Omega(t)$ are the even functions, and the block $\bar{p}(t)\bar{q}(t)$ – is the odd-function, and, therefore, the block $\bar{p}(t)\bar{q}(t)\Omega(t)$ is also the odd function of t. With the help of the symmetry properties of even/odd functions after expanding trigonometric functions and the final integration, the Melnikov function obtains the polyharmonic explicit form depended only on the parameter t_0:

$$M\left(t_0\right) = 2\varepsilon AB \left(\frac{1}{A} - \frac{1}{B} \right) \sum_{n=0}^{N} J_s^{(n)} \left\{ s_n \cos\left(n\omega_p t_0\right) - c_n \sin\left(n\omega_p t_0\right) \right\} \tag{2.15}$$

where

$$J_c^{(n)} = \int_{-\infty}^{+\infty} \bar{p}(t)\bar{q}(t)\Omega(t)\cos\left(n\omega_p t\right) dt = 0; \quad J_s^{(n)} = \int_{-\infty}^{+\infty} \bar{p}(t)\bar{q}(t)\Omega(t)\sin\left(n\omega_p t\right) dt = \text{const}_n \neq 0$$

From the expression (2.15) the fact follows, that the Melnikov function has the infinite set of simple zero-roots and then the perturbed manifolds of the heteroclinic phase-trajectories will be mutually intersecting each other, and will generate the corresponding heteroclinic nets in the phase space, that in its turn inevitably initiates the dynamical heteroclinic chaos.

To confirm the analytically demonstrated fact of the chaos initiation the sections of the perturbed phase space (the Poincaré sections) can be plotted (fig.7). These Poincaré sections were numerically obtained basing on the simple "stroboscopic condition", when the points of the phase trajectories are draw on the common picture at discrete time-moments $t_j = 2\pi j / \omega_p$ multiple of the basic period of the polyharmonic part of perturbation (2.9). All of the Poincaré sections (fig.7) contain the so-called chaotic layers and a great number of new secondary heteroclinic bundles.
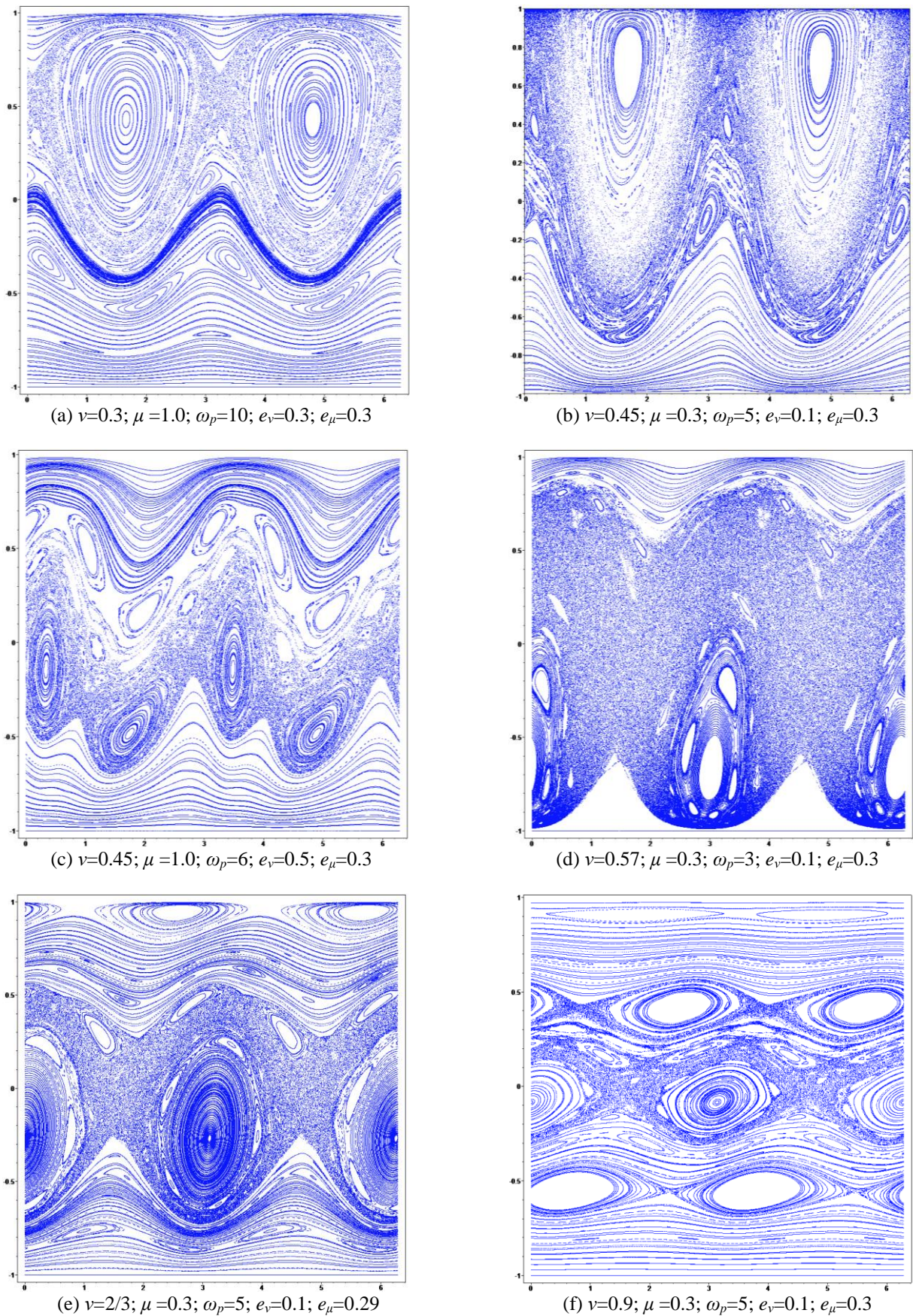
(a) v=0.3; μ =1.0; ω_p=10; e_v=0.3; e_μ=0.3

(b) v=0.45; μ=0.3; ω_p=5; e_v=0.1; e_μ=0.3

(c) v=0.45; μ =1.0; ω_p=6; e_v=0.5; e_μ=0.3

(d) v=0.57; μ =0.3; ω_p=3; e_v=0.1; e_μ=0.3

(e) v=2/3; μ =0.3; ω_p=5; e_v=0.1; e_μ=0.29

(f) v=0.9; μ =0.3; ω_p=5; e_v=0.1; e_μ=0.3

Fig.7 – *The Poincaré sections of the phase space {l, L} of the perturbed system*
A=15, B=10, C_b=6 [kg·m^2]; Δ=3, K=78 [kg·m^2/s]; s_1=1, s_j=c_j=0 (j≠1)

From the form of the Melnikov function (2.13) the possibility of its zero-amplitude follows in some cases. As the trivial example, the zero-amplitude of the Melnikov function appears at the equality of the inertia moments ($A=B$) when the degeneration of the phase portrait occurs, and the dynamical chaos vanishes together with the heteroclinic separatrices.

The second and more interesting example of the Melnikov function with the zero-amplitude can be presented in the case when the condition fulfills:

$$\begin{cases} \Lambda(t) \equiv 0; \\ \Phi = 0 \end{cases} \tag{2.16}$$

The condition (2.16) fulfills, e.g., at the following parametrical combination:

$$\begin{cases} \nu = 2/3; \\ e_\mu = \dfrac{3}{\mu}\left[\dfrac{4}{3}\mu - \dfrac{2}{9}\dfrac{\Delta}{C_b}\right]e_\nu \end{cases} \tag{2.17}$$

In the case (2.17) the integrand in (2.13) becomes equal to zero at all non-zero parameters of the perturbation and at the normal (non-degenerated) form of the phase space (as opposed to the first example with $A=B$). Then the Melnikov function (2.13) has not roots (by t_0). This fact, basing on the Melnikov formalism, could be considered as the condition of the elimination of the chaos, but we regret to note, that this chaos-avoidance-condition (2.17) does not work, and we see as before the chaotic layer near the area of the unperturbed separatrices at the Poincaré map (fig.7-e). So, we must conclude that the simple conditions of the chaos elimination in the considered system cannot be obtained without the additional dissipative torques, which separate the split manifolds of the heteroclinic trajectories with non-zero distance between them.

The Melnikov formalism (as the method developed for the analysis of homoclinic trajectories splitting [30]) is guaranteed to generate the correct anti-chaos conditions only in homoclinic cases and at the detection of non-zero distances between the split manifolds. Some critical aspects relative the Melnikov formalism are indicated in recent works [13, 31], where also the remark is noted, that applying the Melnikov formalism to detecting the "edge of chaos" in heteroclnic cases is far from perfect method [31].

Following to notes [13], it is worth to remind the well-known fact, that at the construction of the Melnikov's formalism [30] the dynamical conditions for the homo/heteroclinic trajectories on infinite limits ($t = \pm\infty$) are very important. In the homoclinic cases these conditions are equal: homoclinic trajectories start and finish in the single original homoclinic point, so the "distances" between the unperturbed original homoclinic point and perturbed one is the same at $t = +\infty$ and at $t = -\infty$. But for heteroclinic cases these dynamical conditions on infinite limits can be differ so far as the heteroclinic trajectories start (at $t = -\infty$) in one point and finish (at $t = +\infty$) in the another point; and, moreover, distances between their unperturbed and corresponding perturbed positions are not obliged to be equal. So, for the heteroclinic cases the guaranteed fulfillment of the Melnikov's formalism is possible at the additional conditions of the equality of distances between unperturbed and perturbed positions of the two different heteroclinic points (e.g. at the "symmetry" of deformations of the split manifolds of

heteroclinic trajectory, and of the whole phase portrait). In the general case for heteroclinic trajectories this additional conditions are not fulfilled *a priori*.

In any case, taking into account the indicated comments, the Melnikov method can be effectively used in tasks of the fundamental detection of the chaos initiation in systems, and also can be applied to obtain the correct conditions of the chaos avoidance.

Conclusion

In the paper the attitude dynamics of the gyrostat-satellite was considered under control by the magnetic actuators in the case of the omega-maneuver implementation and at the presence of additional constant longitudinal component of the magnetic dipole moment of GS. The general and heteroclinic analytical solutions were obtained for the angular motion in conditions of relatively small values of the created magnetic torque (which substantially do not change the direction of the angular momentum vector) and at the coincidence of the external magnetic induction vector and the vector of the angular momentum in the initial time-moment. The phase portrait of the system and its bifurcations were presented. The perturbed dynamics of the GS was considered at the presence of small polyharmonic perturbations in the magnetic dipole moment of the GS was investigated with the help of the Melnikov method and Poincaré sections.

It is quite possible to characterize the studied regimes of the gyrostat angular motion as continuation of the classical tasks of rigid bodies dynamics, especially, the tasks of the heavy tops motion (in Euler's and Lagrange's cases with gyrostatic generalizations), when the restoring/tilting torques act on the gyrostat.

Acknowledgments

References

[1] U.A. Arkhangelskiĭ, Analytical rigid body dynamics. Moscow: Nauka, 1977.

[2] J. Wittenburg, Dynamics of Systems of Rigid Bodies. Stuttgart: Teubner, 1977.

[3] Serret, J. A. (1866), Mémoire sur l'emploi de la méthode de la variation des arbitraires dans la théorie des mouvements de rotation. Mémoires de l'Academie des Sciences de Paris, Vol. 55, pp. 585-616.

[4] Andoyer H. (1923), Cours de Mecanique Celeste, Paris: Gauthier-Villars.

[5] Deprit A. (1967), A free rotation of a rigid body studied in the phase plane, American Journal of Physics 35, pp.424-428.

[6] V.V. Kozlov, Methods of qualitative analysis in the dynamics of a rigid body, Gos. Univ., Moscow, 1980.

[7] V.S. Aslanov, Prostranstvennoe dvizhenie tela pri spuske v atmosfere (Spatial Motion of a Body at Descent in the Atmosphere), Fizmatlit, Moscow, 2004.

[8] V.S. Aslanov, A.V. Doroshin, Chaotic dynamics of an unbalanced gyrostat, Journal of Applied Mathematics and Mechanics (2010), 74 (5), pp. 524-535.

[9] A.V. Doroshin, Exact Solutions in Attitude Dynamics of a Magnetic Dual-Spin Spacecraft and a Generalization of the Lagrange Top, WSEAS Transactions on Systems, Issue 10, Volume 12 (2013) 471-482.

[10] A.V. Doroshin, Chaos and its avoidance in spinup dynamics of an axial dual-spin spacecraft, Acta Astronautica (2014), 94 (2), pp. 563-576.

[11] A.V. Doroshin, Heteroclinic Chaos in Attitude Dynamics of a Dual-Spin Spacecraft at Small Oscillations of its Magnetic Moment, WSEAS Transactions on Systems, Volume 14 (2015) 158-173.

[12] A.V. Doroshin, Heteroclinic Chaos and Its Local Suppression in Attitude Dynamics of an Asymmetrical Dual-Spin Spacecraft and Gyrostat-Satellites. The part I – Main models and solutions, Communications in Nonlinear Science and Numerical Simulation (2016), 31 (1-3), pp. 151-170.

[13] A.V. Doroshin, Heteroclinic Chaos and Its Local Suppression in Attitude Dynamics of an Asymmetrical Dual-Spin Spacecraft and Gyrostat-Satellites. The Part II – The heteroclinic chaos investigation, Communications in Nonlinear Science and Numerical Simulation (2016), 31 (1-3), pp. 171-196.

[14] A. Craig Stickler and K.T. Alfriend, Elementary Magnetic Attitude Control System, Journal of Spacecraft and Rockets, Vol. 13, No. 5 (1976), pp. 282-287.

[15] M. Lovera, A. Astolfi, Spacecraft attitude control using magnetic actuators, Automatica 40 (2004) 1405 – 1414.

[16] E. Silani, M. Lovera, Magnetic spacecraft attitude control: a survey and some new results, Control Engineering Practice 13 (2005) 357–371.

[17] M. Iñarrea, Chaos and its control in the pitch motion of an asymmetric magnetic spacecraft in polar elliptic orbit, Chaos, Solitons & Fractals, Volume 40, Issue 4 (2009) 1637-1652.

[18] V.A. Bushenkov, M. Yu. Ovchinnikov, G.V. Smirnov, Attitude stabilization of a satellite by magnetic coils, Acta Astronautica, Volume 50, Issue 12 (2002) 721-728

[19] M.Yu. Ovchinnikov, D.S. Roldugin, V.I. Penkov, Asymptotic study of a complete magnetic attitude control cycle providing a single-axis orientation, Acta Astronautica 77 (2012) 48–60

[20] M.Yu. Ovchinnikov, A.A. Ilyin, N.V. Kupriynova, V.I. Penkov, A.S. Selivanov, Attitude dynamics of the first Russian nanosatellite TNS-0, Acta Astronautica, Volume 61, Issues 1 (2007) 277-285.

[21] Yan-Zhu Liua, Hong-Jie Yu, Li-Qun Chen, Chaotic attitude motion and its control of spacecraft in elliptic orbit and geomagnetic field, Acta Astronautica 55 (2004) 487 – 494.

[22] Li-Qun Chen, Yan-Zhu Liu, Chaotic attitude motion of a magnetic rigid spacecraft and its control, International Journal of Non-Linear Mechanics 37 (2002) 493–504.

[23] Y.W. Jan, J.C. Chiou, Attitude control system for ROCSAT-3 microsatellite: a conceptual design, Acta Astronautica 56 (2005) 439 – 452.

[24] A.Slavinskis, U.Kvell, E.Kulu, I.Sünter, H.Kuuste, S.Lätt, K. Voormansik, M.Noorma, High spin rate magnetic controller for nanosatellites, Acta Astronautica 95 (2014) 218–226.

[25] F. Bayat H. Bolandi, A.A. Jalali, A heuristic design method for attitude stabilization of magnetic actuated satellites, Acta Astronautica 65 (2009) 1813 –1825.

[26] G. Avanzini and F. Giulietti, Magnetic Detumbling of a Rigid Spacecraft, Journal of Guidance, Control, and Dynamics, Vol. 35, No. 4 (2012), pp. 1326-1334.

[27] Flatley T. et al. A B-dot acquisition controller for the RADARSAT spacecraft //NASA Conference Publication. – NASA, 1997. – pp. 79-90.

[28] A. Zavoli, F. Giulietti, G. Avanzini, G.D.Matteis, Spacecraft dynamics under the action of Y-dot magnetic control law, Acta Astronautica 122 (2016) 146–158.

[29] A.Q. Rogers and R.A. Summers, Creating Capable Nanosatellites for Critical Space Missions //JOHNS HOPKINS APL TECHNICAL DIGEST, VOLUME 29, NUMBER 3 (2010), 283-288.

[30] Melnikov V.K. (1963), On the stability of the centre for time-periodic perturbations, Trans. Moscow Math. Soc. No.12, pp. 1-57.

[31] Xie, J., He, S. H., Liu, Z. H., & Chen, Y. (2017). On Application Melnikov Method to Detecting the Edge of Chaos for a Micro-Cantilever. In "New Advances in Mechanisms, Mechanical Transmissions and Robotics", pp. 155-163. Springer International Publishing.

[32] Zhou, Kaixing, et al. Magnetic attitude control for Earth-pointing satellites in the presence of gravity gradient. Aerospace Science and Technology 60 (2017): 115-123.

[33] Deng, S., Meng, T., Wang, H., Du, C., & Jin, Z. (2017). Flexible attitude control design and on-orbit performance of the ZDPS-2 satellite. Acta Astronautica, 130, 147-161.

[34] Mazzini, L. (2016). Sensors and Actuators Technologies. In Flexible Spacecraft Dynamics, Control and Guidance (pp. 289-324). Springer International Publishing.